Check for updates

Identification of Berbamine, Oxyacanthine and Rutin from *Berberis asiatica* as anti-SARS-CoV-2 compounds: An *in silico* study

Tanuja Joshi [a],[1],[2], Sunaullah Bhat [b],[2], Hemlata Pundir [c], Subhash Chandra [a],*

[a] Computational Biology & Biotechnology Laboratory, Department of Botany, Soban Singh Jeena University, Almora, Uttarakhand, India
[b] Department of Zoology, Kumaun University, S.S.J Campus, Almora, 263601, Nainital, Uttarakhand, India
[c] Department of Botany, D.S.B Campus, Kumaun University, Nainital, 263002, Uttarakhand, India

ABSTRACT

Owing to the shortage of specific medicines, the global pandemic of COVID-19 caused by SARS-CoV-2 has been the greatest challenge for the science community. Researchers from all over the world developed some drugs which failed to completely suppress the contiguous disease. SARS-CoV-2 main protease (Mpro), an important component in viral pathogenesis, is considered as a prospective drug target to stop SARS-CoV-2 infection. Since identification of phytochemicals with anti-Mpro activity has been carried out to develop the potential drugs against SARS-CoV-2. Therefore, the present study was conducted to screen phytochemicals of *Berberis asiatica* for anti-SARS-CoV-2 activity. Through text mining, thirty phytochemicals were reported from *B. asiatica*, of which, three phytochemicals (Berbamine, Oxyacanthine, and Rutin) show high affinity with the SARS-CoV-2 Mpro and exhibited favorable intermolecular interactions with the catalytic residues (His41 and Cys145) and other essential residues. The molecular dynamics simulation showed that Mpro-phytochemical complexes are more stable, less fluctuating, more compact, and moderately extended than the Mpro-X77 (Reference) complex. The number of H-bonds and MMPBSA results also demonstrates that Berbamine, Oxyacanthine, and Rutin are potent Mpro inhibitors having free energy of -20.79, -33.35, and -31.12 kcal mol^{-1} respectively. The toxicity risk prediction supports all phytochemicals for drug-like and non-toxic nature. From the result, we propose that binding of these phytochemicals could hamper the function of Mpro. This work suggests that selected phytochemicals could be used as novel anti-COVID-19 drug candidates, and might act as novel compounds for *in vitro* and in vivo study.

1. Introduction

In December 2019 an unidentified case of pneumonia caused by 2019-nCoV was noticed among some person, in Wuhan city, Hubei Province, China, later on, declared as a global pandemic by the world health organization (WHO) [1–3]. The International Committee on Taxonomy of Viruses (ICTV) and the WHO permanently name the 2019-nCoV pathogen as Severe Acute Respiratory Syndrome Coronavirus 2 (SARS-CoV-2) and the causing disease as Coronavirus disease 2019 (COVID-2019), after whole-genome submitted by different laboratories and regions to GISAID database [4,5]. COVID-19 is a severe and often fatal respiratory tract infection caused by a transmissible human pathogenic SARS-CoV-2. COVID-19 is responsible for medical emergencies

globally as well as in India. While comparing the genomic of SARS-CoV-2, it was found to belong to the Beta coronavirus family and is phylogenetically very similar to SARS-CoV-1, which was accountable for acute pneumonia that occurred in November 2002 in Guangdong Province, China. COVID-19 began in Wuhan in Hubei Province, People's Republic of China, in December 2019, and became a worldwide pandemic [2,3,6]. The infection was extremely contagious which led to the global dissemination of the virus in the following months, thus causing the COVID-19 outbreak [7].

COVID-19 is responsible for a lot of deaths all over the world [8,9]. As per the online data in World meter's report, about 211,487,519 people have been infected with COVID-19, and 4,426,500 deaths occurred at world-wise, till August 20, 2021, (https://www.worldomet

ers.info/coronavirus/), and in India, the cases are increasing on daily basis at an enormous rate with 3,23,92,506 confirmed cases and 4,33, 998 persons being deceased due to COVID-19. As far as India is concerned 57, 22, 81,488 doses of vaccine have been administrated till 20, August 2021 (https://www.COVID19india.org/). With the emergence of the global pandemic of COVID-19, not only the health care system, but the global economy was a decline at an exponential rate. The COVID-19 being a new and largely unknown disease, has provided doctors with the need to investigate and try different methodologies and interventions.

COVID-19 infection causes acute respiratory distress symptoms such as fever, dry cough, and breathing difficulty with an incubation time of around five days (average 2–14 days) [10]. Possible COVID-19 treatments include lopinavir, a coronavirus protease inhibitor [11], ribavirin, a guanosine analog that targets RdRp and was developed to fight the Ebola virus [12], and chloroquine, an antimalarial drug that has displayed antiviral efficacy by disrupting viral fusion with the cell due to increased endosomal pH [13]. In a retrospective study, Xu et al. [3] examined the efficacy of tocilizumab (atlizumab, an immunosuppressive drug) and found that it lowered fever, oxygen requirement, radiological characteristics, and C-reactive protein levels (CRP). Bian et al. [14], in an open-labeled clinical trial (concurrent controlled add-on clinical trial) of meplazumab, identified a median virus clearance rate, discharge time, and improved repair time. The effects of some corticosteroids on coronavirus have also been investigated [15]. Convalescent plasma transplant is still being used now, and it has been shown to lower mortality rates [16]. Two antimalarial agents, chloroquine and hydroxychloroquine's are also being used for emergency coronavirus care [17].

There are currently 172 vaccines in pre-clinical development and 61 vaccines in clinical development, respectively [18]. Some of the most prominent vaccines worldwide are crmirnaty (first vaccine approved by FDA) with an efficacy of about 88% against the delta variant, Spikevav the second vaccine given nods by FDA, GRAd-COV-2, SputnikV (https://www.nytimes.com/interactive/2020/science/coronavirus-vaccine-tracker.htm). Seven vaccines viz., Covaxin, Covishield, SputnikV, ZyCov-D, Moderma mRNA-1273, AD26-COV2.S, AZD 1222 have been given emergency approval for India's immunization program (https://COVID19.trackvaccines.org/country/india/), and of them, the two most commonly used to vaccinate Indian people are Covishield and Covaxin with the effectiveness of 70.42% and 50%, respectively.

To overcome the viral infection, inhibition of replication of the viral genome is a well-known strategy [19]. The virus infection in the host cells can be stopped by inhibiting the cleavage process. Some researchers [20] reported that SARS-CoV-2 genome codes for several non-structural proteins (NSP) including 3-chymotrypsin-like protease (3CLpro), RNA-dependent RNA polymerase (RdRp), and its helicase, papain-like protease (papLpro), the structural glycoprotein, and accessory proteins (12). Among various proteins encoded by SARS CoV-2, Main protease (Mpro) has been reported as a lead potential target for any drug, because it cuts the two replicate polyproteins required to mediate viral replication and transcription [21]. Therefore, Mpro becomes the principal target for drug discovery to identify novel inhibitors of SARS-CoV-2 [21,22]. In a recent study, Nelfinavir was reported to be a COVID-19 drug candidate as the best potential inhibitor of Mpro on the basis of molecular dynamics simulation of docked protein-ligand complex [9,23,24].

As per the WHO report, 80% of the population in developing countries depend on conventional plants for health needs [25]. Herbal medicines which occur naturally offer an extensive variety of natural products, which can serve as a supplementary guide for unscrambling many mysteries behind human illnesses [25,26]. The role of traditional medicine to combat COVID-19 has recently been reported in the literature [3]. Indeed, medicinal plants may be the source of compounds that can have the potential to fight SARS-CoV-2 [27–30].

Berberis asiatica which belongs to the Bereridaceae family has a long history in traditional remedy as the root of *B. asiatica* are used in

indigenous system of medicine for treating various ailments such as rheumatism, jaundice, diabetes, fever, stomach disorders, skin disease, malarial fever, and as a tonic, and so forth [31,32]. It is used as a single plant remedy or in polyherbal formulations, predominantly in specified systems of medicine such as Ayurveda, Siddha, and Unani. This plant has great importance to fight against pneumococcal infection [33]. The major alkaloid of *B. asiatica* has been reported to be berberine ($C20H18NO4+$) [34], which is quaternary ammonium salt from the protoberberine group of isoquinoline alkaloids and is differentially found in the roots, rhizomes, stems, bark, and berries of this plant [28, 35–37]. Different pharmacological properties of berberine including anticonvulsant [38], antidepressant [28,38], anti-Alzheimer [28], anti-arrhythmic [38], anti-inflammatory [38], antiviral [39], antibacterial [39], antineoplastic [35] and anti-diabetic [40,41] have been reported in both in vivo and *in vitro* studies. Berberine besides having anticancer properties, is an essential therapeutic phytochemical agent [28,33] with anti-diabetic, anti-malaria, anti-AIDS, anti-jaundice, anti-cholera, anti-diarrhea, anti-leprosy, and anti-inflammation effects [35,37,42–49].

For drug designing and discovery, the computational technique for screening natural inhibitors is gaining attention among researchers [50]. Researchers have investigated many phytochemicals of known and unknown biological function using computer-based approaches to find out lead compounds that can effectively inhibit the therapeutic targets in SARS-CoV-2 including 3CLpro and PLpro [51,52]. For this, present study was carried out to find out whether *B. asiatica* phytochemicals can also stop viral replication within those infected by SARS-CoV-2or not, therefore virtual screening was carried out to find out potential natural anti-SARSCoV-2 agents. Therefore, Main Protease (306 amino acids) was adopted as a target which is essential for the survival and function of polypeptide generation in the host cell. In order to find novel SARS-CoV-2 Mpro inhibitors, researchers studied the docking score of *B. asiatica* phytochemicals with SARS-CoV-2 Mpro using text mining, molecular docking, molecular dynamics simulation, drug-likeness, and toxicity prediction approaches. Furthermore, we also investigated the *in-silico* toxicity of the screened phytochemicals.

2. Materials and methods

2.1. Literature review and phytochemical dataset preparation

B. asiatica was undertaken in this study due to its various therapeutic roles against several diseases. Text mining analysis showed that various phytochemicals of *B. asiatica* have antiviral properties. Hence to screen antiviral compounds against SARS-CoV-2, a dataset of *B. asiatica* phytochemicals was built in-house by collecting information from the scientific literature. DLAD4U (Disease List Automatically Extracted For You), PubTator, and Carrot2 servers were used for creating a dataset of *B. asiatica* phytochemicals by text mining analysis. The scientific name of the plant (*B. asiatica*) and COVID-19 were used as keywords for the search. The pieces of literature cited were focused largely on the COVID-19 resources that were made publicly available to the science community (COVID-19 open research dataset https://pages.semanticscholar.org/coronavirus-research), but also on specific databases such as Pubmed and Google scholar. Here, we conducted molecular docking of *B. asiatica* phytochemicals with SARS-CoV-2 Mpro to screen antiviral phytochemicals against coronavirus.

2.2. Molecular docking

A) Protein preparation: More than a dozen proteins are encoded by the SARS-CoV-2 genome, the most studied of which is the 3CLpro. The main enzyme of the SARS-CoV-2 virus is a protease (Mpro or 3CLpro) which is vital CoV enzyme and plays a significant role in promoting viral replication and transcription, thus making it a most critical drug target [21]. The Mpro crystal structures (PDB ID: 6W63) attached with its

inhibitor (X77) was collected from the Protein Data Bank and imported into the PyMol to visualize the binding domain and to identify the amino acids in the binding site pocket. The protein was added with hydrogen atoms to fix the ionization and tautomeric states of the amino acids using the AutoDockTools (ADT). Furthermore, prior to the docking, the water molecules and ligand bound to the receptor molecule were eliminated by utilizing PyMol. In addition, the protein was subjected to energy minimization by using the AMBER 14SB force field with a maximum number of 200 steps at 0.02 RMS gradients. The optimized protein structure was then saved in pdbqt format and imported to PyRx for molecular docking.

A) Ligand preparation: The X77 (N-(4-tertbutylphenyl)-N-[(1R)-2-(cyclohexylamino)-2-oxo-1-(pyridin-3-yl) ethyl]-1H-imidazole-4-carboxamide) was used as reference compound in this study. The three-dimensional (3D) structure of the X77 co-crystallized with Mpro was retrieved for the respective protein structure from Protein Data Bank [http://www.rcsb.org/pdb/home/home.do]. PubChem database were used to retrieve the SDF files of each phytochemical (http://pubchem.ncbi.nlm.nih.gov/). The files were converted into a PDB file using the OpenBabel tool [53]. The Polar hydrogen charges were assigned and the non-polar hydrogens were integrated by using ADT [54]. Finally, for docking the reference ligand (X77), as well as other ligands (phytochemicals), were converted to pdbqt format.

A) Molecular docking studies: Molecular docking was performed using AutoDock Vina [55] once the target and ligands were prepared. The potential to estimate the scoring function and analysis of protein-ligand interactions to figure out the ligand's binding affinity and activity determination is the foremost objective of molecular docking [56]. Autodock Vina in the PyRx platform was used to generate the binding pose of phytochemicals in the active site of SARS-CoV-2 Mpro. The amino acid residues of Mpro interacting with their co-crystallized ligand i. e. X77 was taken as the active site residues and docking grid parameters were set accordingly (Fig. 1C). The active site pocket contains amino acid residues Thr25, Thr26, His41, Phe140, Leu141, Asn142, Gly143, Ser144, Cys145, His163, His164, Met165, Glu166, Asp187, and Gln189. The parameters for the grid box were set as x, y, z size, and center coordinates: −20.11, 18.79, - 27.35, and 25, 25, and 25 respectively.

B) Validation of the docking protocol: The validation of the docking procedure was carried out by docking the co-crystallized ligand at the active site of Mpro. The docking algorithm was then carried out by keeping the exhaustiveness 8. Hit phytochemicals with the lowest binding energy (kcal/mol) than X77 and anticipated interactions with the essential amino acids present at the active site of the protein can exhibit powerful antagonist properties against SARS-CoV-2 Mpro. The program Discovery studio visualizer was used to visualize hydrogen and hydrophobic contacts at the SARS-CoV-2 Mpro inhibitor site.

2.3. Molecular dynamics (MD) simulation

MD simulation was implemented to validate the docking analysis and quantify the change in protein conformation. The MD simulation
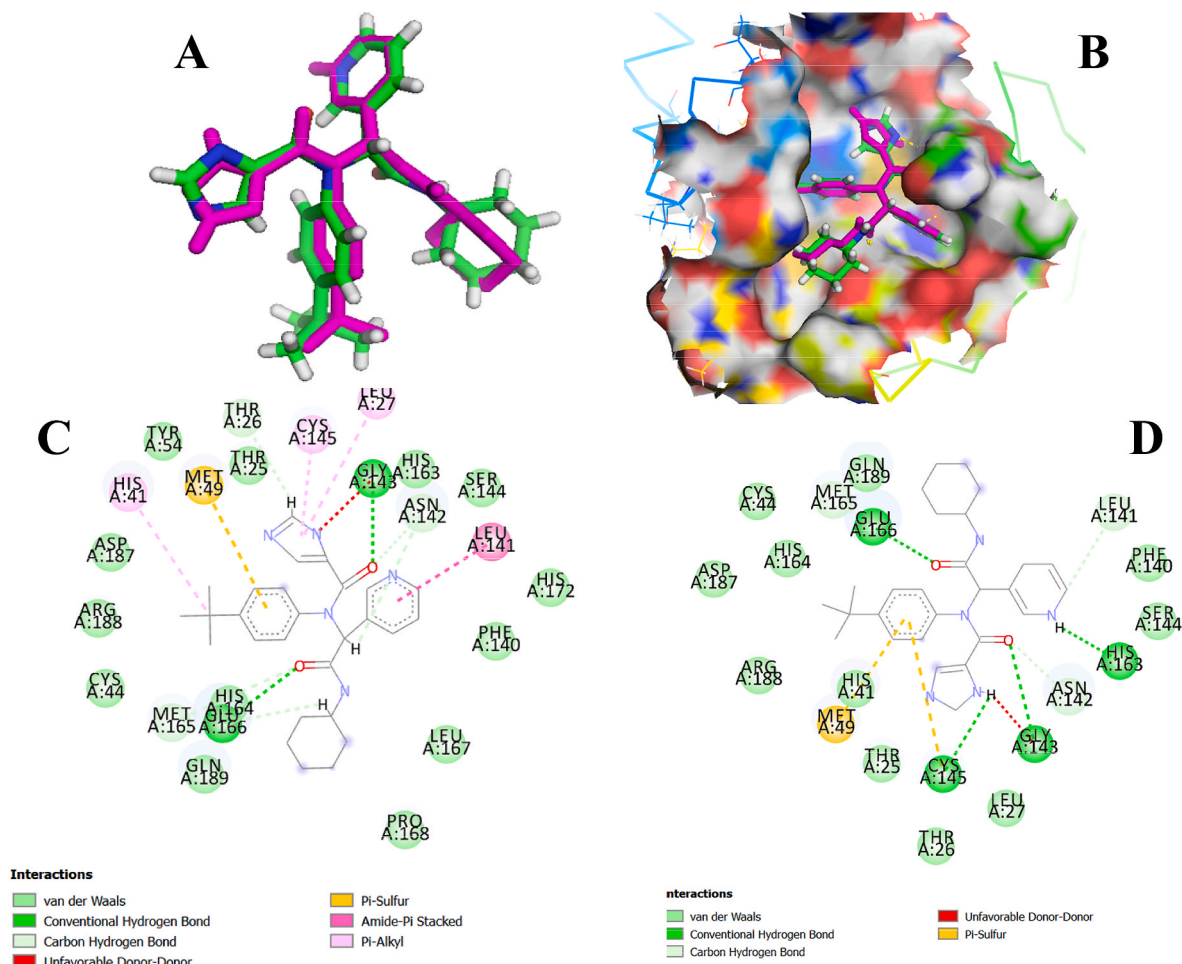

Fig. 1. The figure showing superimposition of the docked and experimental structure of X77 where green and magenta color represent experimental and docked molecule respectively (A), superimposition of both structure at the active site of Mpro (B) and 2D interaction of experimental X77 (C) and docked X77 (D) with the active site residues of Mpro.

package GROMACS 5.0.7 [57] was used to simulate the systems (protein-ligand complex and apo-protein structure) wherein the CHARMM 36 force field was used for building the topology of each system [58]. Using transferable intermolecular potential water molecules (TIP3P-model) [59], the water molecules were added, and then neutralization of the system was achieved by adding 4 Na ions at a temperature of 310 K. For energy minimization of the system, the periodic boundary condition was retained where the Particle Mesh Ewald (PME) approach [60] with the steepest descent algorithm was used for the measurement of long-range electrostatic interaction using the Verlet cutoff scheme at 10 kJ mol^{-1}. A dodecahedral simulation box was developed to simulate the system that was 10 Å greater than the size of system. The Berendsen thermostat [61] has been used to monitor the temperature of the simulation system. Initially, each system were cleaned and equilibrated in two stages by the steepest gradient approaches [62] (5000 ps); NVT and NPT ensemble.

Lastly, constant temperature and pressure of 300 K and 1 atm, were maintained for all the systems subjected to the production MD of 250 ns. The simulation time was maintained using the Parrinello–Rahman with a time step of 2fs for constant pressure simulation. To evaluate the result, the simulation trajectory was saved for every 100 ps.

The MD simulation results were incorporated with the GROMACS default script. Finally, MD trajectories were evaluated for the measurement of Root-mean-square-deviation (RMSD), Root-mean-square-fluctuation (RMSF), Radius-of-gyration (Rg), Solvent-accessible-surface-area (SASA) [63], Hydrogen bonds (H-bonds), and principal component analysis (PCA) (http://thegrantlab.org/bio3d_v2/tutorials/principal-component-analysis) [64]. This was worked out to measure the strength of the protein-ligand interaction. The researcher also calculated the non-bonded interaction energy between protein and ligands with the same parameter as MD simulation. In order to get a more accurate MD simulation result, each complex was run three times (n = 3) and the average result was used for analysis.

To calculate the binding free energy, the molecular mechanics Poisson–Boltzmann surface area (MMPBSA) approach was used [65]. The MD trajectories were processed before doing MMPBSA calculations. Binding free energy calculations include free solvation energy (polar + nonpolar solvation energies) and potential energy (electrostatic energies + van der Waals interactions). In the following equation, the whole process of MMPBSA can be summarized:

$$\Delta G_{bind} = \Delta G_{complex\ (minimized)} - [\Delta G_{ligand\ (minimized)} + \Delta G_{receptor\ (minimized)}]$$

$$\Delta G_{bind} = \Delta G_{MM} + \Delta G_{PB} + \Delta G_{SA} - T\Delta S$$

Here, the sum of van der Waals and electrostatic interaction is ΔG_{MM}, the polar and non-polar solving energies are ΔG_{PB} and ΔG_{SA} respectively, and the entropic contribution is $T\Delta S$. For average binding energy measurements, the 'python' script provided in g_mmpbsa was used. The last 10 ns MD trajectory files were considered for the MM-PBSA measurement.

2.4. Toxicity prediction

The phytochemicals with better binding energy and stability with the Mpro receptor were taken for the detailed toxicity analysis using the OSIRIS Property Explorer [66]. OSIRIS open-source software was used to predict the risk of drug toxicity for properties like tumorigenicity, mutagenicity, reproductive development, irritation, and drug score.

3. Results

3.1. Antiviral potential of B. asiatica

Text mining analysis using various servers (PubMed, Carrot2, and DLAD4U) was done to commence studies in different research papers. A total of 30 phytochemicals of *B. asiatica* were collected from various pieces of literature. Table 1 provides the name of the phytochemicals and the details of the publication. Data from text mining revealed that several pharmacological effects like antimicrobial, hepto-protective, anti-diabetic, antioxidant, anti-diarrheal, anti-inflammatory, cardiotonic, ophthalmic, skin related problems, laxative, anti-depressant, immune-modulatory, anti-tumor, neuro-protective, antifungal, and potential antiviral activities are found in *B. asiatica*. The plants belong to the genus Berberis have many medicinal properties due to the presence of alkaloids with different pharmacological activities [67]. The antiviral potential of *B. asiatica* is may be due to the antiviral activity present on various secondary metabolites (phytochemicals) of the plant. Out of 30 phytochemicals found in *B. asiatica*, 21 phytochemicals show the antiviral activity against a total of 31 different viruses (Herpes simplex virus (HSV-1, HSV-2), Adenovirus, Zika virus (ZIKV), Hepatitis C virus (HCV), Human papillomavirus (HPV), Hepatitis B virus (HBV), West Nile virus (WNV), Chikungunya virus (CHIKV), Porcine reproductive and respiratory syndrome virus (PRRS), Human Immunodeficiency Virus (HIV-1), Ebola virus, Influenza A, Influenza B, SARS-CoV-1, Poliovirus (PV-1), Rhinovirus (HRV, HRV-2, HRV-3, HRV-4), Tobacco mosaic virus (TMV), Cucumber mosaic virus (CMV), Respiratory syncytial virus (RSV), Enterovirus71 (EV71), Dengue virus (DENV), Human cytomegalovirus (HCMV), SARS-CoV-2, MERS-CoV, Parainfluenza-III, Yellow fever virus, and Japanese encephalitis virus (JEV) (Table 1).

Table 1 suggests that *B. asiatica* phytochemicals can be used to develop antiviral drugs for the treatment of COVID-19.

3.2. Molecular docking of B. asiatica phytochemicals with the Mpro

The virtual screening of all *B. asiatica* phytochemicals was performed by the molecular docking approach at the active sites of Mpro using the PyRx tool. The coordinate center and size of the target protein (Mpro) were generated from the center of mass of its standard inhibitor (X77), which was estimated by using the "centerofmass" function of PyMOL.

Validation of the docking protocol: The protocol of molecular docking was validated by docking the reference ligand/standard inhibitor X77 into the active site of Mpro, before doing the virtual screening. The docked X77 was superimposed to compare with experimental X77 (Fig. 1A and B). To validate docking, the RMSD value was calculated. The RMSD value amid the experimental and docked reference molecule X77 was 0.653 angstrom, which is perfectly acceptable. The result displayed that the docked X77 exhibited well-established hydrogen bonds and hydrophobic bonds with similar amino acid residue as the experimental X77 formed with the active pocket of the receptor (Fig. 1C and D). The figure also indicates the formation of four conventional hydrogen bonds with Glu166, His163, Gly143, and Cys145; three carbon-hydrogen interactions with Met165, Leu141, and Asn142; eleven van der Waals interaction with Phe140, Ser144, Leu27, Thr26, Thr25, His41, Arg188, Asp187, His164, Cys44, and Gln189; three unfavorable donor-donor interaction with Gly143, and Pi-sulfur bond with Met49 in Mpro-docked X77 (Fig. 1D). Since our docking protocol produced a similar docked pose for X77 as found in the crystal structure of Mpro, the protocol was considered satisfactory and could reliably be used for the docking of the compounds of interest.

Molecular docking: Further, molecular docking studies were carried out between receptor SARS-CoV-2 Mpro and ligand (*B. asiatica* phytochemicals) using AutoDock Vina. All the 30 phytochemicals were analyzed for the binding energy with Mpro. Table 2 consists of name of all phytochemicals with their molecular formula, and binding energies (kcal mol^{-1}) with SARS-CoV-2 Mpro. After successfully docking these phytochemicals with target Mpro, the result shows 8 different poses of receptor-ligand interactions for each ligand. The compounds with docking scores less than the reference molecule were regarded as compounds of interest as they are the most stable ligands in comparison to the reference ligand. The frequency graph of all the docked compounds is given in Fig. 2. Docking results revealed that all 30 phytochemicals

Table 1

List of all phytochemicals of *B. asiatica* with their anti-viral effect.

S. No.	Phytochemicals	References	PubChem Id	Antiviral activity against
1	Berbamine	[68]	CID: 275182	DENV [69], EV-71 [69], JEV [69], MERSCoV [69], SARSCoV-1 [70], ZIKV [69], and SARSCoV-2 [71]
2	Oxyacanthine	[68]	CID: 442333	SARSCoV-1 ACE2 [70] and SARSCoV-2 ACE2 [72]
3	Rutin	[73]	CID: 5280805	EV-71 [74] and HIV-1 [74]
4	Pakistanamine	[75]	CID: 193238	–
5	Phloridzin	[73]	CID: 6072	–
6	Protoberberine	[75]	CID: 114943	–
7	Stigmasterol	[75]	CID: 5280794	HSV-1 [76]
8	Berberine	[68]	CID: 2353	CHIKV [77], EV-71 [3], HCMV [78,79], HIV-1 [80], HPV [79], HSV-1 [79], and HSV-2 [79]
9	Berberrubine	[75]	CID: 72704	–
10	Ketoberberine	[75]	CID: 11066	–
11	Catechin	[73]	CID: 9064	Adenovirus [81], CHIKV [81], Ebola virus [81], HBV [81], HCV [81], HIV-1 [81], HPV [81], HSV-1 [81], Influenza A [81], PRRS [81], SARSCoV1 [70], WNV [81], and ZIKV [81]
12	Chlorogenic acid	[73]	CID: 1794427	Adenovirus [14], HBV [14], HIV-1 [14], HSV-1 [27], HSV-2 [27], and Influenza A [14]
13	Columbamine	[68]	CID: 72310	HIV-1 [82]
14	Magnoflorine	[75]	CID: 73337	HIV-1 [83] and HSV-1 [84]
15	Ellagic acid	[73]	CID: 5281855	DENV [85], Ebola virus [86], HIV-1 [4], HPV [87], HRV-2 [4], HRV-3 [4], and HRV-4 [4]
16	Jatrorrhizine	[68]	CID: 72323	HIV-1 [83]
17	Palmatine	[68]	CID: 19009	DENV [11], HIV-1 [82], RSV [4], SARSCoV-1 [70], WNV [11], Yellow fever virus [11], and ZIKV [88]
18	Dihydropalmatine	[75]	CID: 1023495	–
19	Ferulic acid	[73]	CID: 445858	CMV [2] and TMV [2]
20	Xanthophyll	[89]	CID: 5281243	–
21	Alpha-carotene	[89]	CID: 4369188	–
22	Gallic acid	[73]	CID: 370	EV-71 [4], HCV [90], HIV-1 [91], HSV-1 [91], HSV-2 [91,92], Influenza A [4], Influenza B [4], Parainfluenza-III [93], and SARSCoV-1 [70]
23	Caffeic acid	[73]	CID: 689043	HSV-1 [94], Influenza A [94], PV-1 [94], and SARSCoV-1 [70]
24	M-coumaric acid	[73]	CID: 637541	–
25	Coumarin	[95]	CID: 323	SARS-CoV-1 [70]
26	Beta-carotene	[89]	CID: 5280489	HIV-1 [96] and SARSCoV-1 [70]
27	3-Hydroxybenzoic acid	[73]	CID: 7420	HRV [97]

Table 1 (*continued*)

S. No.	Phytochemicals	References	PubChem Id	Antiviral activity against
28	P-coumaric acid	[73]	CID: 637542	HRV-2 [98], HRV-3 [98], HRV-4 [98], RSV [7], and SARSCoV-1 [70]
29	Vanillic acid	[73]	CID: 8468	HSV-1 [99], HSV-2 [99], and SARSCoV-1 [70]
30	Ascorbic acid	[89]	CID: 54670067	Influenza A [4] and SARSCoV-1 [70]

Table 2

B. asiatica phytochemicals, Molecular Formula and score obtained from molecular docking.

S. No.	Phytochemicals	Molecular Formula	Docking score (kcal mol^{-1})
1	X77 (Reference)	C27H33N5O2	−8.4
2	Berbamine	C37H40N2O6	−9.7
3	Oxyacanthine	C37H40N2O6	−8.5
4	Rutin	C27H30O16	−8.4
5	Pakistanamine	C38H42N2O6	−8.3
6	Phloridzin	C21H24O10	−8.2
7	Protoberberine	C17H14 N+	−8.1
8	Stigmasterol	C29H48O	−7.7
9	Berberine	C20H18NO4+	−7.6
10	Berberrubine	C19H16NO4+	−7.6
11	Ketoberberine	C20H17NO5	−7.6
12	Catechin	C15H14O6	−7.5
13	Chlorogenic acid	C16H18O9	−7.5
14	Columbamine	C20H20NO4+	−7.5
15	Magnoflorine	C20H24NO4+	−7.5
16	Ellagic acid	C14H6O8	−7.5
17	Jatrorrhizine	C20H20NO4+	−7.2
18	Palmatine	C21H22NO4+	−7.1
19	dihydropalmatine	C21H23NO4	−6.9
20	Ferulic acid	C10H10O4	−6
21	Xanthophyll	C40H56O2	−5.9
22	alpha-carotene	C40H56	−5.9
23	Gallic acid	C7H6O5	−5.8
24	Caffeic acid	C9H8O4	−5.8
25	m-coumaric acid	C9H8O3	−5.8
26	coumarin	C9H6O2	−5.8
27	beta-carotene	C40H56	−5.7
28	3-Hydroxybenzoic acid	C7H6O3	−5.6
29	p-coumaric acid	C9H8O3	−5.6
30	Vanillic acid	C8H8O4	−5.1
31	ascorbic acid	C6H8O6	−4.9

had binding energy between the range of −4 kcal mol^{-1} to −9 kcal mol^{-1}, which was lower or equivalent to binding energy the reference (X77) (−8.4 kcal mol^{-1}).

Berbamine showed the strongest affinity to Mpro while ascorbic acid showed the weakest binding energy. Three phytochemicals of *B. asiatica* (Berbamine, Oxyacanthine, and Rutin) show their inhibitory action by representing a lower binding energy score (higher docking scores) compared with the binding energy of X77 (−8.4 kcal mol^{-1}). Berbamine, Oxyacanthine, and Rutin were found to bind at the active site of Mpro with docking scores of −9.7 kcal mol^{-1}, -8.5 kcal mol^{-1}, and -8.4 kcal mol^{-1} respectively (Table 2). The molecular docking result suggested that screened compounds may have the same mechanism of action as the reference molecule. Therefore, it is quite evident that screened phytochemicals from *B. asiatica* have good potential against Mpro. Then, all these three compounds along with X77 were further used for molecular interaction analysis of protein-ligand complex.

The 2D interactions of the screened phytochemicals, as well as reference ligand X77, were visualized by Discovery studio visualizer. From molecular docking analysis, a total of 30 compounds were
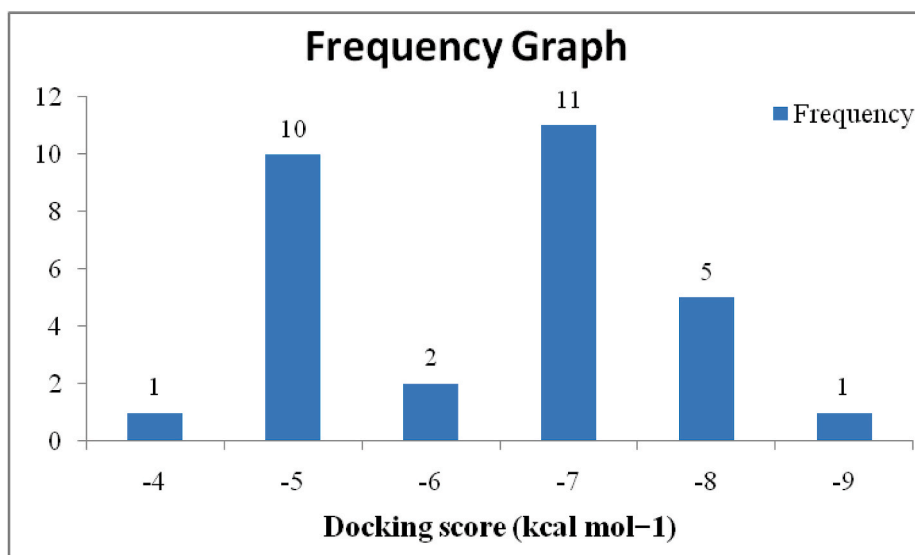
Fig. 2. Frequency distribution graph of 30 docked compounds over the range of docking scores.

screened and following best three docked compounds with their receptor-ligand 2D interaction images are shown in Fig. 3. The active site residues include Thr25, Thr26, Leu27, His41, Cys44, Met49, Tyr54, Phe140, Leu141, Asn142, Gly143, Ser144, Cys145, His163, His164, Met165, Glu166 Leu167, Pro168, His172, Asp187, Arg188, and Gln189 (Fig. 1C). Table 3 showed necessary H-bond formation with possible active residues by ligands required for the inhibition of SARS-CoV-2 Mpro.

The binding profile of the Mpro-Berbamine complex revealed mainly van der Waals interaction with Leu167, Glu166, Leu141, Asn142,

Gly143, Arg188, Gln 189, Gln 192, and Thr190; while Met165 was involved in hydrogen bond formation with the sulfur group. Hydrophobic interaction was also predominant in the binding of Berbamine to Mpro such as π-alkyl interaction with Pro168, Met49, His41, and Cys145 and Alkyl bond with His41, Met49, and Cys44 (Fig. 3A). Catalytic residues Met165, His41, Cys145, and Pro168 were visualized in hydrophobic interaction (π-alkyl) with Oxyacanthine where a single Conventional and Carbon hydrogen bonds were also observed with Thr190 and Asn142 respectively. Leu141, Gly143, Thr25, Cys25, Arg188, Gln192, Gln189, and Glu166 were involved in van der Waals
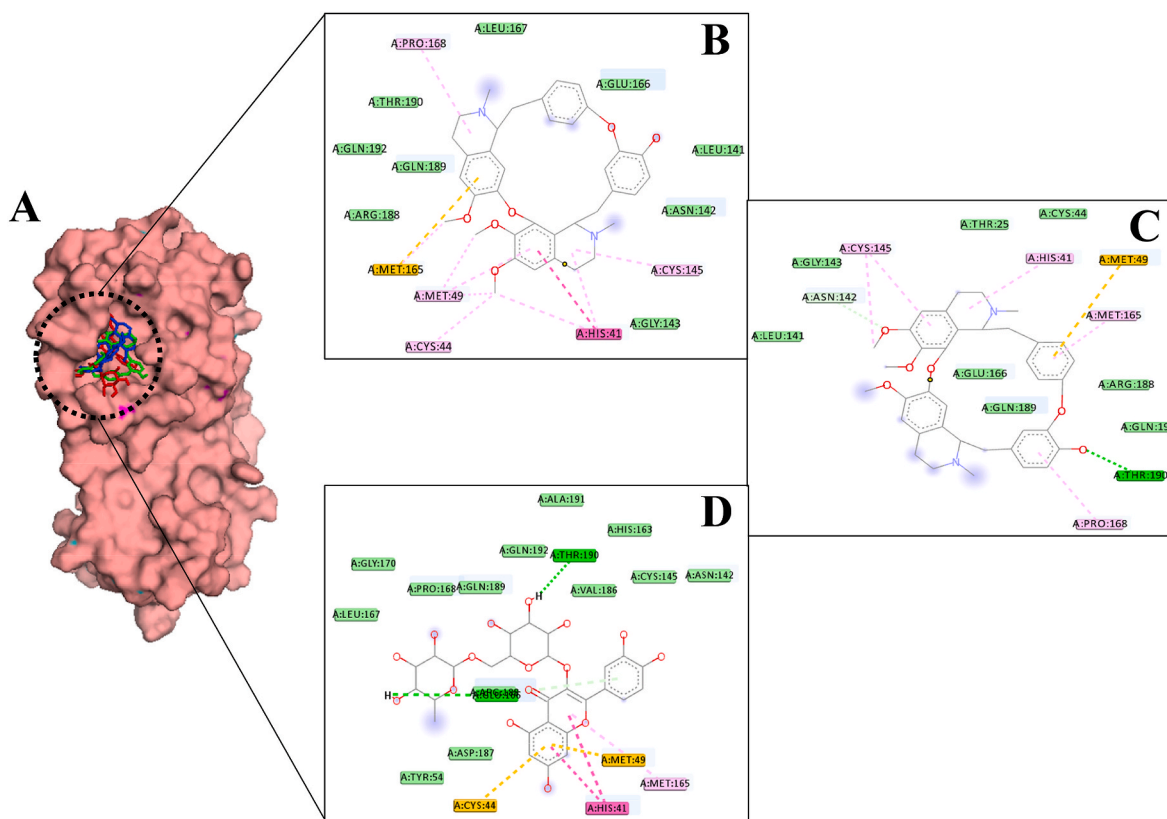

Fig. 3. Binding of Mpro-phytochemical complexes, (a) binding of Berbamine, (b) Oxyacanthine, and (c) Rutin to the active site of Mpro.

Table 3

Hydrogen and Non-Hydrogen bond interaction between Screened phytochemicals and Mpro.

S. No.	Ligands	Van der Waals interaction	Conventional hydrogen interaction	Carbon hydrogen interaction	Unfavorable donor-donor interaction	Pi-sulfur interaction	Pi-pi stacked interaction	Pi-alkyl interaction	Alkyl interaction
1	X77 (Reference)	Phe140, Ser144, Leu27, Thr26, Thr25, His41, Arg188, Asp187, His164, Cys44, Gln189	Glu166, His163, Gly143, Cys145	Met165, Leu141, Asn142	Gly143	Met49			
2	Berbamine	Leu167, Glu166, Leu141, Asn142, Gly143, Arg188, Gln189, Gln192, Thr190				Met165		Pro168, Met49,His41, Cys145	His41, Met49, Cys44
3	Oxyacanthine	Leu141, Gly143, Thr25, Cys25, Arg188, Gln192, Gln189, Glu166	Thr190	Asn142	–	Met49		Met165, His41, Cys145, Pro168	Cys145
4	Rutin	Asp187, Thr54, Leu167, Gly170, Pro168, Gln189, Gln 192, Ala191, Val186, His163, Cys145, Asn142	Thr190, Arg188	Glu166		Cys44, Met49	His41	Met165	

interactions Cys145 was linked via Alkyl bond while Met49 was involved in hydrogen bond formation with the sulfur group in the Mpro-Oxyacanthine complex (Fig. 3B). As visualized with Discovery studio, Met165 was involved in hydrophobic interactions (Pi-alkyl bond) while His41 was linked via π-π stacking in Rutin. Two conventional hydrogen bonds with Thr190 and Arg188, and a single Carbon hydrogen bond with Glu166 was also observed in Rutin's binding to Mpro protein. In addition, van der Waals interactions were formed with Asp187, Thr54, Leu167, Gly170, Pro168, Gln189, Gln 192, Ala191, Val186, His163, Cys145, and Asn142, while Cys44 and Met49 were involved in hydrogen bond formation with the sulfur group (Fig. 3C).

From this study, it can be seen that all screened compounds, as well as reference, are generally interacted with the same residues i.e. His41, Met49, Cys145, Met165, Glu166, and Gln189, which are well known to be involved in the active site of Mpro. All these screened phytochemicals showed novel hydrogen and hydrophobic bonding interactions with active residues of the target protein. In comparison with the reference molecule, they showed lower docking scores and also have shown stronger interactions with the target protein and thus, these phytochemicals may be considered as potential inhibitors of Mpro.

The docked Mpro-ligand complexes were subsequently used to study the detailed dynamic, structural, as well as binding behaviors by MD simulations which allow investigating how the ligands interact with SARS-CoV-2's active site.

3.3. Structural stability, fluctuation and compactness of Mpro-ligand complexes during MDS

The MD simulation trajectories of 250 ns simulations were examined to study the detailed structural and dynamic mechanisms of the Mpro protein and Mpro-ligand complexes. The RMSD, RMSF, and Rg fluctuations profile of all systems during the period of 250 ns simulation are presented in Figs. 4–6. The RMSD of the backbone atoms computed over 250 ns revealed that the Mpro protein reached stability after approximately 50 ns, whereas all the Mpro-ligand complexes took only 5–10 ns to become stable (Fig. 4). Mpro-X77 complex as well as all the Mpro-phytochemical complexes were stabilized until the end of the MD production run and converged overall except Mpro-Oxyacanthine complex which is stable up to 200 ns and after that, it showed a little fluctuation of about 0.1 ns and become stable immediately after this. The RMSD plot suggested that the last 10 ns were most preferable for further structural and dynamics analyses as all the complexes were stable during this time. The average RMSD values of Mpro, Mpro-X77 complex, Mpro-Berbamine complex, Mpro-Oxyacanthine complex, and Mpro-Rutin complex were found to be 0.20 ± 0.03 nm, 0.22 ± 0.04 nm, 0.16 ± 0.02 nm, 0.18 ± 0.01 nm, and 0.19 ± 0.05 nm, respectively.
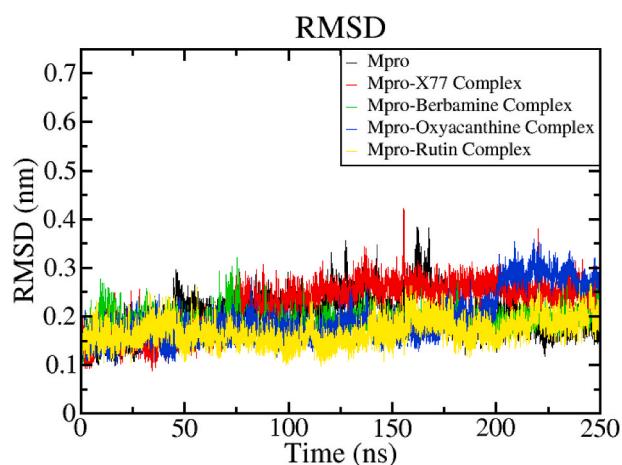

Fig. 4. RMSD analysis of the plot of Mpro and Mpro-ligand complexes during MD simulation.
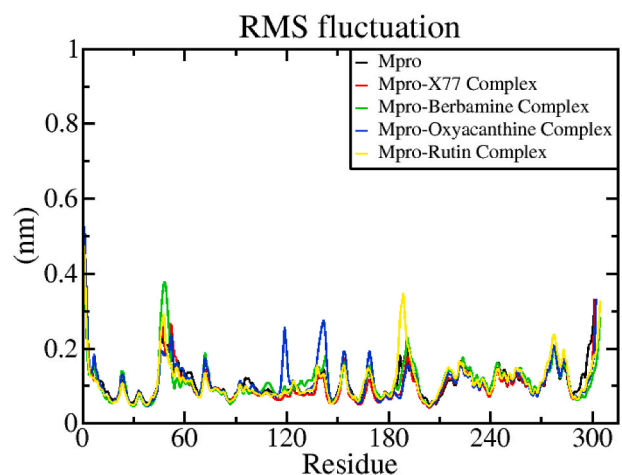

Fig. 5. RMSF analysis plot of residues of Mpro and Mpro-ligand complexes during MD simulation.

Interestingly, the RMSD values of all the systems were very similar and do not exceed 0.4 nm, which denotes the structural integrity of the Mpro protein. The RMSD profile suggested that upon phytochemical binding no significant variation or conformational changes were taking place in
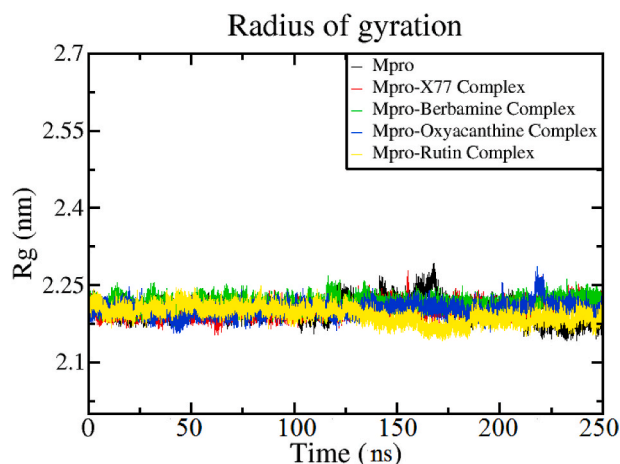
Fig. 6. Radius of gyration analysis plot of Mpro and Mpro-ligand complexes during MD simulation.

Fig. 7. Hydrogen bond analysis plot of protein-ligand complexes during MD simulation.

the Mpro structure.

The structural flexibility was evaluated by the residue-wise RMSF in Mpro protein and Mpro-ligand complexes. RMSF specifies the flexible region of the protein and analyzes the portion that diverges from the overall structure. A higher RMSF value indicates greater flexibility (less stability) during the MD simulation while the lower value of RMSF suggests less flexibility (good stability) of the system. All the Mpro-phytochemical complexes exhibited overall similar or lower RMSF values than the Mpro-X77 complex during the simulation (Fig. 5). RMSF analysis suggests that all active site residues had fluctuation less than 0.2 nm and were found to be stable throughout the simulation period, which is completely acceptable.

The Rg of the protein and protein-ligand complex indicates the degree of compactness and rigidity of the protein. Therefore, the Rg values of Mpro and Mpro-ligand complexes were investigated to evaluate their compactness during the 250ns simulation run. For this, we have calculated the Rg of Mpro and Mpro-ligand complexes during the 250 ns simulation time. The average Rg values of Mpro and Mpro-X77 complex were found to be 1.84 ± 0.22 nm and 1.73 ± 0.27 nm respectively. Similarly, Rg values were found to be 1.71 ± 0.29 nm, 1.73 ± 0.24 nm, and 1.70 ± 0.25 nm for the Mpro-Berbamine complex, Mpro-Oxyacanthine complex, and Mpro-Rutin complex, respectively, but in the case of the Mpro-Oxyacanthine complex little fluctuation was observed in between 220 ns and 225 ns. From Rg profiles, it was observed that the Mpro-ligand complex exhibited a more compact behavior than the Mpro protein without ligand and Mpro-X77 complex.

The lower RMSD, reduced residue-wise fluctuation, and higher compact nature in the Mpro phytochemical complexes are indicating their overall stability as well as convergence.

3.4. H-bonds, solvent-accessible area, and Gibbs free energy analyses of Mpro-phytochemical complexes

H-bonds are essential for drug specificity, metabolization, and stability. H-bond analysis of Mpro-ligand complexes performed was for the period of 250 ns simulation to understand the H-bond and its contributions to the overall stability of the system as shown in Fig. 7. The Mpro-Rutin complex was the only one that formed a maximum of nine H-bonds while maintaining an average of five. The binding pocket residues i.e. His41, Asn142, Glu166, Gln189, Thr190, and Gln192 were involved in H-bond formation. The average H-bonds in the Mpro-Oxyacanthine complex was three, while the maximum had reached four. Gly143, Arg188, Thr190, and Gln192 were the binding site residues that had formed H-bonds with this complex. The highest H-bonds formed by the Mpro-Berbamine complex was five, and the average H-
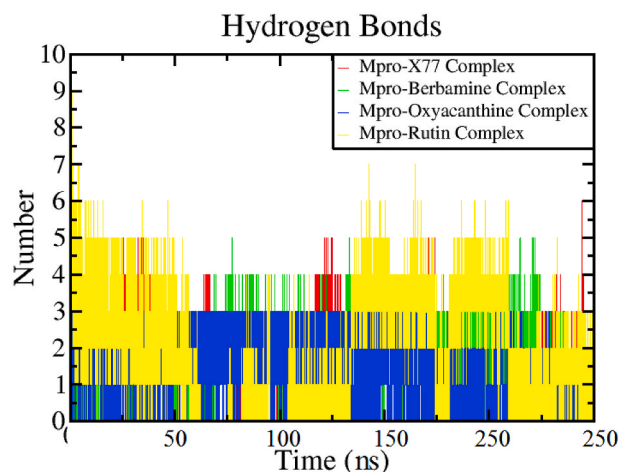
bonds formed was four. This complex formed a H-bond with the residues Glu166, Asp187, Gln189, and Thr190, which are involved in binding at the active site of Mpro protein. The Mpro-X77 complex had formed a maximum of six H-bond, with an average of three H-bonds. The binding site residues Asn142, Gly143, Ser144, Cys145, His163, and Glu166 of Mpro protein had formed H-bond with the complex. After analyzing results, it was found that all Mpro-phytochemical complexes did not deviate and almost similar numbers of H-bonds were formed between Mpro-phytochemical complexes and Mpro-X77 complex, indicating that all phytochemicals were bound to the Mpro as closely and effectively as its standard inhibitor X77. During the 250 ns simulation run, all complexes were found stable and observed within the pocket. This suggests that H-bonds probably played an important role in the stability of the Mpro-X77 complex during the MD simulation, and also indicates stability to the Mpro-phytochemical complexes.

Fig. 8 showed that the SASA of Mpro-X77 complex and Mpro-phytochemical complexes. The average SASA values were found to be 152.58 ± 2.89 nm^2 for the Mpro-Berbamine complex, 152.03 ± 2.80 nm^2 for the Mpro-Oxyacanthine complex, and 151.16 ± 2.95 nm^2 for Mpro-Rutin complex respectively. The Mpro-X77 complex showed the average SASA value of 150.35 ± 2.86 nm^2. However, after 40 ns Mpro-X77 complex as well as all the Mpro-phytochemical complexes showed almost similar surface area (Fig. 8). The results showed a similar assessable surface area of phytochemicals to the reference X77 in the aqueous system, which indicates equivalent
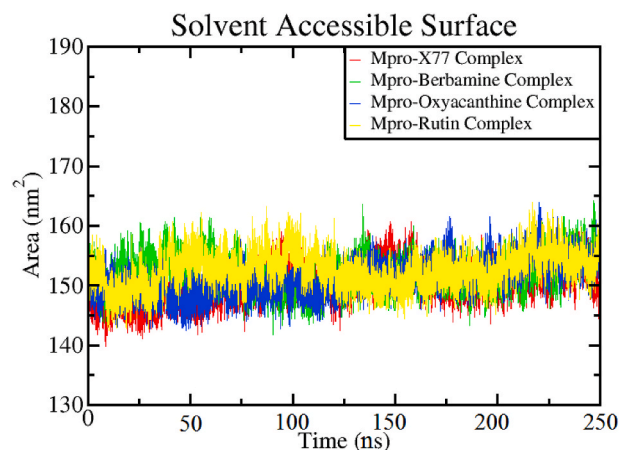

Fig. 8. MD simulation result showing fluctuations in the solvent accessibility surface area during the simulation period.

stability of phytochemicals with Mpro as X77.

PCA represents the average variation in motion within the protein on ligand binding as compared to the free protein [100]. ED allows the interpretation of dominant and collective modes from the overall dynamics of the MD trajectory. FEL denotes the probability of energy distribution as a function of one or more collective variables of the protein [101,102]. Gibb's free energy landscape (FEL) also predicted the stability of each protein-ligand complex. Using the g_sham tool of the GROMACS package, the FEL (ΔG) was generated from PC1 and PC2 projections and are shown in Fig. 9. In these plots, ΔG values ranging from 0 to 15.7 kcal mol^{-1}, 0–15.8 kcal mol^{-1}, 0–15 kcal mol^{-1}, and 0–14.3 kcal mol^{-1} for Mpro-X77 complex, Mpro-Berbamine complex, Mpro-Oxyacanthine complex, and Mpro-Rutin complex respectively. All the Mpro-phytochemical complexes represent similar or lower energies as compared to the Mpro-X77 complex, which indicates that these phytochemicals follow the energetically more favorable transitions during the MDS.

3.5. Binding free energy calculations in Mpro-phytochemical complexes

To determine how firmly phytochemicals bind to Mpro and their respective binding modes, the binding free energies were calculated using the MM-PBSA approach. The MD trajectories were analyzed through MM-PBSA to know the binding free energy values and their energy components. For this purpose, the last 10 ns trajectories were investigated to calculate binding energies and insights into the binding modes of phytochemicals with Mpro. Four different energy components were used to calculate the binding free energy: electrostatic, van der Waals, polar solvation, and SASA energies. The binding free energy was calculated for all protein-ligand complexes and is shown in Table 4. The reference molecule X77 was found to display binding energy of -17.59 ± 3.32 kcal mol^{-1} for Mpro. Computation of the binding energies of phytochemicals for the Mpro revealed that Berbamine, Oxyacanthine, and Rutin had the binding energy -20.79 ± 16.07 kcal mol^{-1}, -33.35 ± 15.28 kcal mol^{-1}, and -31.12 ± 2.57 kcal mol^{-1} respectively. The detailed study of the individual energy components revealed that all components including the van der Waals energy, Electrostatic Energy, and SASA energy, except the polar solvation energy contributed to the efficient binding of phytochemicals with Mpro. In all the studied complexes the major contributing energy was van der Waals energy.

Although all complexes were bound in the same binding pocket of the enzyme, variations in energy contribution of each residue may be a major factor in the difference in binding free energy. For the last 10 ns of
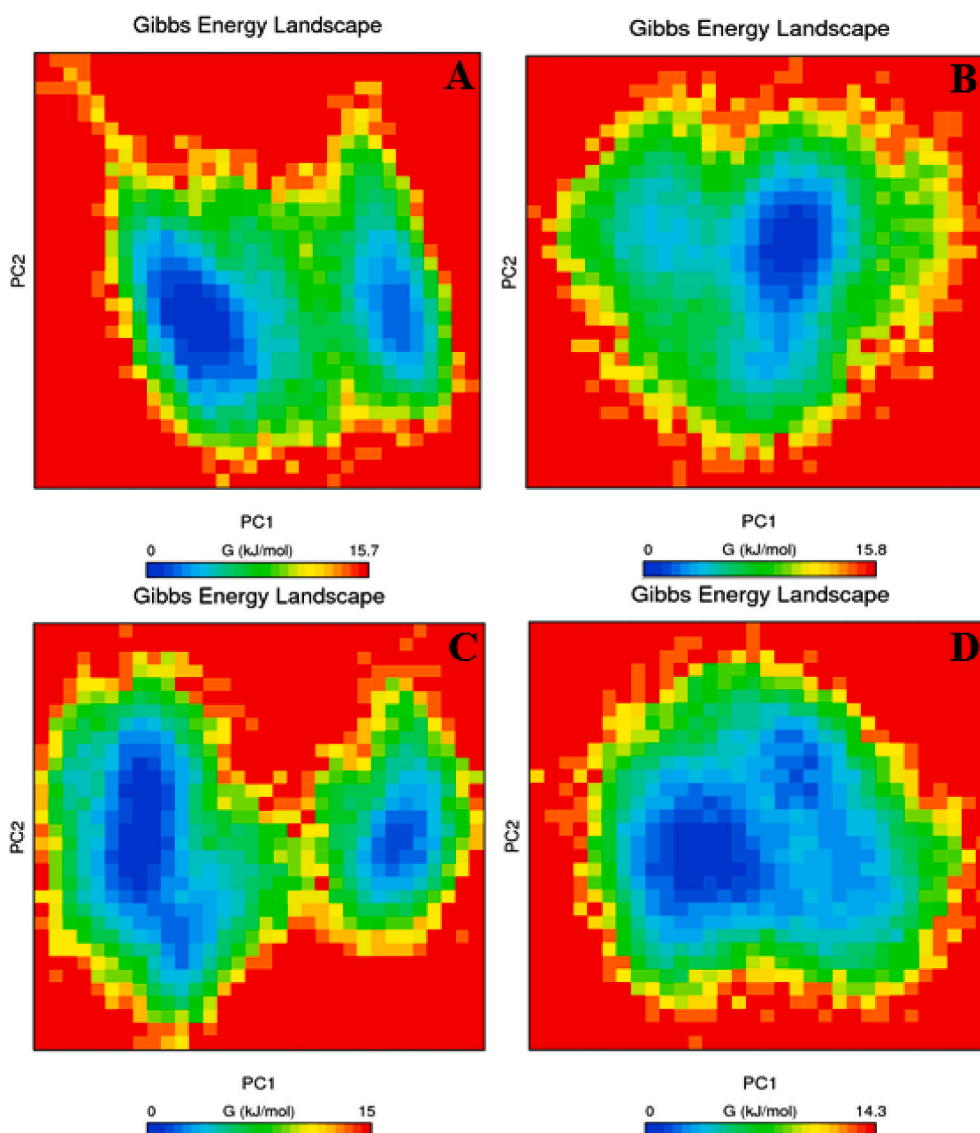

Fig. 9. PCA-DeltaG plot of (A) Mpro-X77 complex, (B) Mpro-Berbamine complex, (C). Mpro-Oxyacanthine complex, and Mpro-Rutin complex.

Table 4

Table showing the binding free energy and its energy components of Mpro-X77 complex and Mpro-phytochemical complexes from the MDS trajectory.

S No.	Protein/Protein-ligand complex	van der Waals Energy (kcal mol^{-1})	Electrostatic Energy (kcal mol^{-1})	Polar salvation energy (kcal mol^{-1})	SASA energy (kcal mol^{-1})	Binding Energy (kcal mol^{-1})
1	Mpro-X77 complex	−41.15 ± 3.15	−11.96 ± 3.35	40.25 ± 4.75	−4.75 ± 0.29	−17.59 ± 3.32
2	Mpro-Berbamine complex	−26.93 ± 2.75	−11.71 ± 4.55	21.20 ± 16.99	−3.35 ± 0.41	−20.79 ± 16.07
3	Mpro-Oxyacanthine complex	−24.40 ± 5.18	−8.11 ± 2.41	2.33 ± 14.88	−3.18 ± 0.68	−33.35 ± 15.28
4	Mpro-Rutin complex	−49.47 ± 2.77	−5.55 ± 1.51	28.91 ± 1.98	−5.00 ± 0.22	−31.12 ± 2.57

MD simulation trajectories, a per residue interaction energy profile was also developed using the MM-PBSA approach to identify the essential residues involved in ligand binding with Mpro protein. Fig. 10 shows a per-residue decomposition plot of the total binding energy of the Mpro-ligand complexes. Only residues that contribute most to overall binding energy are illustrated in the figure for a better representation of the results. The plot showed that the major contributing amino acids in all complexes were Thr25, Leu27, His41, Cys44, Met49, Cys145, Met165, Asp187, and Gln189. The per-residue interaction plot revealed that the majority of residues had negative binding energy, while only a few had positive binding energy. The residues with negative binding energy were important in maintaining the stability of protein-ligand complex. When compared to other active site residues, Met49, Cys145, and Met165 play the most significant roles in Mpro-ligand stabilization. The contribution of the binding energy of each residue was different in each complex which had made a large difference in the final binding energy of each complex. The higher energy contribution from the binding site residues in case of Mpro-phytochemical complexes explains the stability of the complex.

The results of binding free energy calculations and other previous MD simulation (RMSD, RMSF, RG, H-Bond, and SASA analysis) led to the conclusion that Berbamine, Oxyacanthine, and Rutin had better stability and binding energy towards the Mpro as compared to its standard inhibitor X77.

3.6. Toxicity prediction of screened compound

The US Food and drug administration's toxicity risk predictor tool OSIRIS was used to predict molecular properties and toxicity of phytochemicals [66]. In addition to the drug-likeness properties including cLogP, LogS (solubility), MW, and drug-like properties, OSIRIS also predicted the various toxicity risk properties such as tumorigenicity (TUMO), mutagenicity (MUT), irritation (IRRI), and reproductive development (REP) toxicity. The results of OSIRIS prediction for Berbamine, Oxyacanthine, and Rutin are summarized in Table 5. The drug score shows ranges between 0 and 1, where the value 1 indicates the good possibility of a compound to be a drug molecule, whereas, the score value 0 indicates that compounds having no possibilities of being a drug candidate. The result of toxicity estimation shows that reference molecules, X77 as well as Berbamine, Oxyacanthine, and Rutin have no risk of any kind of toxicity i.e. they all are non-reproductively toxic, non-irritating, non-tumorigenic, and non-mutagenic. Thus, considering the toxicity prediction results, we suggest that these three screened phytochemicals i. e. Berbamine, Oxyacanthine, and Rutin can be exploited as promising drug candidates for the development of anti-SARS-COV-2 drug molecules.

Table 5

Toxicity profile of screened phytochemicals.

S. No.	Ligand	Drug score	MUT	TUMO	IRRI	REP
1	Reference (X77)	0.31	Non-toxic	Non-toxic	Non-toxic	Non-toxic
2	Berbamine	0.21	Non-toxic	Non-toxic	Non-toxic	Non-toxic
3	Oxyacanthine	0.21	Non-toxic	Non-toxic	Non-toxic	Non-toxic
4	Rutin	0.57	Non-toxic	Non-toxic	Non-toxic	Non-toxic
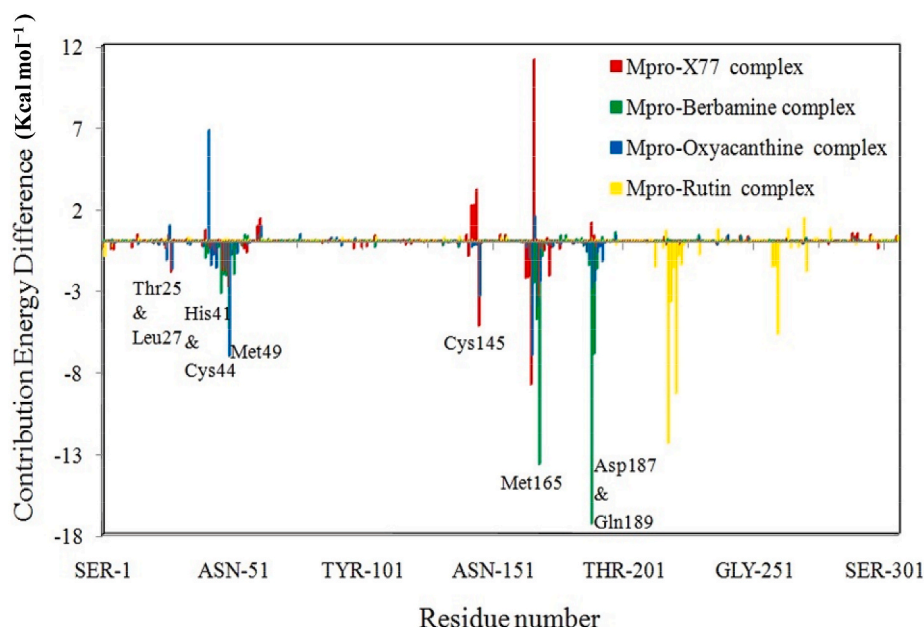
Fig. 10. Analysis of binding free energy contribution of each residue in Protein-ligand complexes during MD simulation.

4. Discussion

The effective drugs and vaccines search against SARS-CoV-2 is the most urgent and challenging task for global researchers at this moment. Currently, synthetic antiviral drugs used to treat COVID-19 such as lopinavir/ritonavir [103,104] and remdesivir [104] as well as some antimalarial drugs like hydroxychloroquine and chloroquine [104] have various side effects, and therefore, there is a great need to explore the natural resources which can boost immunity as well as cure viral disease. The practice of natural extracts from medicinal plants in the prevention of COVID-19 is highly inspired by the previous SARS treatments. According to the many reports, several plants metabolites possess the potential antiviral activity and therefore, they may be used as natural therapeutics for the treatment of COVID-19 Pandemic [88,105]. Recent studies by Joshi et al. reported the beneficial role of natural compounds from lichen and plants against COVID-19 [27,106].

One of the most well-known plants with various pharmacological properties is *B. asiatica*. To find out potential compounds against COVID-19, *B. asiatica* was selected in this study. *B. asiatica* is known for its diversity and pharmacological uses in the traditional medicine system since the ancient times [107]. Several investigations have supported the traditional role of *B. asiatica*. This is one of the plants used in Ayurveda and the Yunani medicine system for curing jaundice, eyesores, toothache, asthma, and skin pigmentation; drying unhealthy ulcers; like a fomentation for removing inflammation and swelling [32].

In this study of drug discovery, 30 phytochemicals were investigated from *B. asiatica*. these phytochemicals were verified for their against any potential viral disease. Thus, these compounds were explored in PubMed and DLAD4U for text mining analysis and it was found that many phytochemicals of *B. asiatica* show antiviral properties. Table 1 illustrates the list of phytochemicals of *B. asiatica* which are effective against various viral diseases. Then, the antiviral network of *B. asiatica* phytochemicals revealed that the 21 phytochemicals out of 30 were found to have effective inhibitory activity against a total of 31 viruses and each phytochemical is effective against more than one virus. The ability of phytochemicals to inhibit a broad spectrum of viruses may be useful in the treatment of SARS-CoV-2. Therefore, to find out potential anti-SARS-CoV-2 compounds, a phytochemical dataset of *B. asiatica* was prepared. These 30 phytochemicals were subjected to molecular docking against Mpro of SARS-CoV-2. Based on the molecular docking score of 30 phytochemicals, the three phytochemicals, viz. Berbamine, Oxyacanthine, and Rutin were screened which showed good binding energy with SARS-CoV-2 Mpro.

Further MD simulations were carried out on Berbamine, Oxyacanthine, and Rutin phytochemicals complexed with Mpro. The conformational changes and stability of all the Mpro-phytochemicals complexes were analyzed by RMSD, RMSF, RGS SASA, and H-bond analysis, etc from MD simulation trajectories. All these phytochemicals have shown good results and stability throughout the 250 ns simulation period. RMSD result indicates that all the phytochemicals possess better stability towards the active site of Mpro as compared to the reference, X77. RMSF analysis represents the lower atomic fluctuations in binding residues of Mpro indicating small conformation changes in Mpro after binding phytochemicals. Various MD simulation results revealed that all Mpro-phytochemicals complexes were highly stable throughout the 250 ns MD simulation run.

To validate the docking score, binding free energy calculations were performed using the last 10 ns of MD simulation trajectories. During the last 10 ns, all complexes show stable trajectories, and therefore last 10 ns trajectories were used for binding free energy calculations. The Mpro-Berbamine, Mpro-Oxyacanthine, and Mpro-Rutin complexes showed excellent binding free energy and the result of all the complexes was better than the reference, Mpro-X77 Complex. The least binding free energy indicates that Berbamine, Oxyacanthine, and Rutin can act in a significant way against the Mpro. Toxicity analysis demonstrated that these phytochemicals did not have a risk of any kind of toxicity and can

be used as a drug with the value of tolerance prescribed for human consumption. The study also shows that all the screened phytochemicals also have drug scores similar to the reference and could be utilized as drug candidates against COVID-19.

The two screened phytochemicals of *B. asiatica* viz. Berbamine and Oxyacanthine are already reported to show effectiveness against the ACE-2 target of SARS-CoV-2 [71,72] but, still, there is no such report against the Mpro target of SARS-CoV-2. Interestingly, the current findings emphasize that both these phytochemicals Berbamine and Oxyacanthine are also effective against Mpro. Hence, it suggests that these phytochemicals can prevent the replication of SARS-CoV-2 by targeting both ACE-2 as well as Mpro and consequently prevent the pathogenesis. Hence, these phytochemicals are likely to be developed as an orally active drug candidates.

5. Conclusion

The outbreak of COVID-19 is caused rapid deaths across the globe caused and has imposed great concern on the scientific community to develop potential drugs against it. Plants have been the natural source of the healthcare system since ancient times. SARS-CoV-2 uses Mpro to mediate the process of its replication and transcription. Targeting Mpro can lead to such changes in structural conformation in the virus which stops its replication and transcription inside the host cells. In this study, the *in silico* approach was applied for drug discovery in order to identify specific potential natural candidates to stop viral replication within those infected by SARS-CoV-2. Here, the phytochemicals of *B. asiatica* against SARS-CoV-2 Mpro were explored. In this research, for the first time various phytochemicals from *B. asiatica* were reported for their anti-SARS-CoV-2 activity, specifically by targeting the Mpro receptor. Molecular docking, MD simulation, binding free energy analysis indicate that three Phytochemicals viz. Berbamine, Oxyacanthine, and Rutin are not only bound strongly with the Mpro but also stabilized the 3D conformations of the protein structure after binding. Furthermore, the drug-score and toxicity profile of all phytochemicals showed their promising therapeutic potential. The results reveal that compounds from *B. asiatica* could have antiviral activity against SARS-CoV-2 and other viral diseases. Thus, Berbamine, Oxyacanthine, and Rutin from the *B. asiatica* and other *Berberis* species can surely be evaluated further *in vitro* and clinical trials to evaluate their antiviral potential.

Data availability statement

All the data cited in this manuscript is generated by the authors and available upon request from the corresponding author.

Declaration of competing interest

The authors declare that they have no known competing financial interests or personal relationships that could have appeared to influence the work reported in this paper.

infrastructure to establish Bioinformatics Centre in Kumaun University, S.S.J Campus, Almora.

References

[1] N.C. Peeri, N. Shrestha, M.S. Rahman, R. Zaki, Z. Tan, S. Bibi, et al., The SARS, MERS and novel coronavirus (COVID-19) epidemics, the newest and biggest global health threats: what lessons have we learned? Int. J. Epidemiol. 49 (2020) 717–726.

[2] E. Long, H. Lin, Z. Liu, X. Wu, L. Wang, J. Jiang, et al., An artificial intelligence platform for the multihospital collaborative management of congenital cataracts, Nat. Biomed. Eng. 1 (2017) 1–8.

[3] X. Xu, M. Han, T. Li, W. Sun, D. Wang, B. Fu, et al., Effective treatment of severe COVID-19 patients with tocilizumab, Proc. Natl. Acad. Sci. Unit. States Am. 117 (2020) 10970–10975.

[4] S. Jeon, M. Ko, J. Lee, I. Choi, S.Y. Byun, S. Park, et al., Identification of antiviral drug candidates against SARS-CoV-2 from FDA-approved drugs, Antimicrob. Agents Chemother. 64 (2020) e00819–e00820.

[5] C. Liu, Q. Zhou, Y. Li, L.V. Garner, S.P. Watkins, L.J. Carter, et al., Research and Development on Therapeutic Agents and Vaccines for COVID-19 and Related Human Coronavirus Diseases, ACS Publications, 2020.

[6] N.C. Peeri, N. Shrestha, M.S. Rahman, R. Zaki, Z. Tan, S. Bibi, et al., The SARS, MERS and novel coronavirus (COVID-19) epidemics, the newest and biggest global health threats: what lessons have we learned? Int. J. Epidemiol. (2020).

[7] M. Giovanetti, D. Benvenuto, S. Angeletti, M. Ciccozzi, The first two cases of 2019-nCoV in Italy: where they come from? J. Med. Virol. 92 (2020) 518–521.

[8] O. World Health, Statement on the Second Meeting of the International Health Regulations (2005) Emergency Committee Regarding the Outbreak of Novel Coronavirus (2019-nCoV), 2020.

[9] O. World Health, WHO Director-General's Remarks at the Media Briefing on 2019-nCoV on 11 February 2020, 2020.

[10] B.S. Kamps, C. Hoffmann, COVID reference. Tradução de Joana Catarina Ferreira da Silva e Sara Mateus Mahomed. Alemanha, Steinhäuser Verlag, 2020.

[11] T.T. Yao, J.D. Qian, W.Y. Zhu, Y. Wang, G.Q. Wang, A systematic review of lopinavir therapy for SARS coronavirus and MERS coronavirus-A possible reference for coronavirus disease-19 treatment option, J. Med. Virol. 92 (2020) 556–563.

[12] D. Falzarano, E. De Wit, A.L. Rasmussen, F. Feldmann, A. Okumura, D.P. Scott, et al., Treatment with interferon-α2b and ribavirin improves outcome in MERS-CoV-infected rhesus macaques, Nat. Med. 19 (2013) 1313–1317.

[13] M.J. Vincent, E. Bergeron, S. Benjannet, B.R. Erickson, P.E. Rollin, T.G. Ksiazek, et al., Chloroquine is a potent inhibitor of SARS coronavirus infection and spread, Virol. J. 2 (2005) 1–10.

[14] H. Bian, Z.-H. Zheng, D. Wei, Z. Zhang, W.-Z. Kang, C.-Q. Hao, et al., Meplazumab Treats COVID-19 Pneumonia: an Open-labelled, Concurrent Controlled Add-on Clinical Trial, 2020. MedRxiv.

[15] C.D. Russell, J.E. Millar, J.K. Baillie, Clinical evidence does not support corticosteroid treatment for 2019-nCoV lung injury, Lancet 395 (2020) 473–475.

[16] J. Mair-Jenkins, M. Saavedra-Campos, J.K. Baillie, P. Cleary, F.-M. Khaw, W. S. Lim, et al., The effectiveness of convalescent plasma and hyperimmune immunoglobulin for the treatment of severe acute respiratory infections of viral etiology: a systematic review and exploratory meta-analysis, J. Infect. Dis. 211 (2015) 80–90.

[17] T.E. Tallei, S.G. Tumilaar, N.J. Niode, B.J. Kepel, R. Idroes, Y. Effendi, et al., Potential of plant bioactive compounds as SARS-CoV-2 main protease (Mpro) and spike (S) glycoprotein inhibitors: a molecular docking study, Scientifica (2020) 2020.

[18] S. Kashte, A. Gulbake, S.F. El-Amin Iii, A. Gupta, COVID-19 vaccines: rapid development, implications, challenges and future prospects, Hum. Cell (2021) 1–23.

[19] E. De Clercq, P. Herdewijn, Strategies in the design of antiviral drugs, Pharmaceut. Sci. Encycl.: Drug Discov. Dev. Manuf. (2020) 1–56.

[20] S. Boopathi, A.B. Poma, P. Kolandaivel, Novel 2019 coronavirus structure, mechanism of action, antiviral drug promises and rule out against its treatment, J. Biomol. Struct. Dyn. (2020) 1–10.

[21] K. Anand, J. Ziebuhr, P. Wadhwani, J.R. Mesters, H. R, Coronavirus main proteinase (3CLpro) structure: basis for design of anti-SARS drugs, Science 300 (2003) 1763–1767.

[22] J. Ziebuhr, Structure of coronavirus main proteinase reveals combination of a chymotrypsin fold with an extra alpha-helical domain, EMBO J. 21 (2002) 3213–3224.

[23] F. Musarrat, V. Chouljenko, A. Dahal, R. Nabi, T. Chouljenko, S.D. Jois, et al., The anti-HIV drug nelfinavir mesylate (Viracept) is a potent inhibitor of cell fusion caused by the SARSCoV-2 spike (S) glycoprotein warranting further evaluation as an antiviral against COVID-19 infections, J. Med. Virol. 92 (2020) 2087–2095.

[24] G. Bolcato, M. Bissaro, M. Pavan, M. Sturlese, S. Moro, Targeting the coronavirus SARS-CoV-2: computational insights into the mechanism of action of the protease inhibitors lopinavir, ritonavir and nelfinavir, Sci. Rep. 10 (2020) 1–8.

[25] R.K. Ganjhu, P.P. Mudgal, H. Maity, D. Dowarha, S. Devadiga, S. Nag, et al., Herbal plants and plant preparations as remedial approach for viral diseases, Virus Dis. 26 (2015) 225–236.

[26] G. Mahady, Global Harmonisation of Herbal Health Claims, 2001.

[27] T. Joshi, T. Joshi, P. Sharma, S. Mathpal, H. Pundir, V. Bhatt, et al., In silico screening of natural compounds against COVID-19 by targeting Mpro and ACE2 using molecular docking, Eur. Rev. Med. Pharmacol. Sci. 24 (2020) 4529–4536.

[28] R.S. Joshi, S.S. Jagdale, S.B. Bansode, S.S. Shankar, M.B. Tellis, V.K. Pandya, et al., Discovery of potential multi-target-directed ligands by targeting host-specific SARS-CoV-2 structurally conserved main protease, J. Biomol. Struct. Dyn. 39 (2021) 3099–3114.

[29] M.T. Khan, A. Ali, Q. Wang, M. Irfan, A. Khan, M.T. Zeb, et al., Marine natural compounds as potents inhibitors against the main protease of SARS-CoV-2–a molecular dynamic study, J. Biomol. Struct. Dyn. (2020) 1–11.

[30] R. Islam, M.R. Parves, A.S. Paul, N. Uddin, M.S. Rahman, A.A. Mamun, et al., A molecular modeling approach to identify effective antiviral phytochemicals against the main protease of SARS-CoV-2, J. Biomol. Struct. Dyn. 39 (2021) 3213–3224.

[31] G. Watt, Economic products of India exhibited in the economic court, in: Calcutta International Exhibition, L883-84: Medicinal Products, Superintendent of Government Print, 1883.

[32] K. Kirtikar, B.D. Basu, Indian medicinal plants, Indian Med. Plants (1998).

[33] D.K. Bhandari, G. Nath, A.B. Ray, P.V. Tewari, Antimicrobial activity of crude extracts from Berberis asiatica stem bark, Pharmaceut. Biol. 38 (2000) 254–257.

[34] D.S. Bhakuni, A. Shoeb, S.P. Popli, Studies in Medicinal Plants: Part 1-Chemical Constituents of Berberis Asiatica Roxb, 1968.

[35] F. Cheng, W. Li, Y. Zhou, J. Shen, Z. Wu, G. Liu, et al., admetSAR: a Comprehensive Source and Free Tool for Assessment of Chemical ADMET Properties, ACS Publications, 2012.

[36] J.-P. Hu, K. Nishishita, E. Sakai, H. Yoshida, Y. Kato, T. Tsukuba, et al., Berberine inhibits RANKL-induced osteoclast formation and survival through suppressing the NF-kappaB and Akt pathways, Eur. J. Pharmacol. 580 (2008) 70–79.

[37] K.H. Janbaz, A.H. Gilani, Studies on preventive and curative effects of berberine on chemical-induced hepatotoxicity in rodents, Fitoterapia 71 (2000) 25–33.

[38] M. Imenshahidi, H. Hosseinzadeh, Berberis vulgaris and berberine: an update review, Phytother Res. 30 (2016) 1745–1764.

[39] Y.L. Siow, L. Sarna, O. Karmin, Redox regulation in health and disease—Therapeutic potential of berberine, Food Res. Int. 44 (2011) 2409–2417.

[40] J. Yin, H. Zhang, J. Ye, Traditional Chinese medicine in treatment of metabolic syndrome. Endocrine, metabolic & immune disorders-drug targets (formerly current drug targets-immune, Endocrine Metabol. Disord. 8 (2008) 99–111.

[41] Tabeshpour, J., Imenshahidi, M., Hosseinzadeh, H. A review of the effects of Berberis vulgaris and its major component, berberine, in metabolic syndrome. Iran. J. Basic Med. Sci.. 20, 557.

[42] D. Popov, Novel protein tyrosine phosphatase 1B inhibitors: interaction requirements for improved intracellular efficacy in type 2 diabetes mellitus and obesity control, Biochem. Biophys. Res. Commun. 410 (2011) 377–381.

[43] A. Caraballo, B. Caraballo, A. Rodríguez-Acosta, Preliminary assessment of medicinal plants used as antimalarials in the southeastern Venezuelan Amazon, Rev. Soc. Bras. Med. Trop. 37 (2004) 186–188.

[44] I.L. Lu, N. Mahindroo, P.H. Liang, Y.H. Peng, C.J. Kuo, K.C. Tsai, et al., Structure-based drug design and structural biology study of novel nonpeptide inhibitors of severe acute respiratory syndrome coronavirus main protease, J. Med. Chem. 49 (2006) 5154–5161.

[45] J. Villinski, E. Dumas, H.-B. Chai, J. Pezzuto, C. Angerhofer, S. Gafner, Antibacterial activity and alkaloid content of Berberis thunbergii, Berberis vulgaris and Hydrastis canadensis, Pharmaceut. Biol. 41 (2003) 551–557.

[46] J.-M. Hwang, C.-J. Wang, F.-P. Chou, T.-H. Tseng, Y.-S. Hsieh, W.-L. Lin, et al., Inhibitory effect of berberine on tert-butyl hydroperoxide-induced oxidative damage in rat liver, Arch. Toxicol. 76 (2002) 664–670.

[47] F.R. Stermitz, P. Lorenz, J.N. Tawara, L.A. Zenewicz, K. Lewis, Synergy in a medicinal plant: antimicrobial action of berberine potentiated by 5'-methoxyhydnocarpin, a multidrug pump inhibitor, Proc. Natl. Acad. Sci. Unit. States Am. 97 (2000) 1433–1437.

[48] N. Ivanovska, S. Philipov, Study on the anti-inflammatory action of Berberis vulgaris root extract, alkaloid fractions and pure alkaloids, Int. J. Immunopharm. 18 (1996) 553–561.

[49] M. Chopra, A. Chatterji, S. Pakrashi, The Treatise on Indian Medicinal Plants, CSIR, New Delhi, 1981, pp. 33–35.

[50] I. Aanouz, A. Belhassan, K. El-Khatabi, T. Lakhlifi, M. El-Ldrissi, M. Bouachrine, Moroccan Medicinal plants as inhibitors against SARS-CoV-2 main protease: computational investigations, J. Biomol. Struct. Dyn. (2020) 1–9.

[51] K. Chojnacka, A. Witek-Krowiak, D. Skrzypczak, K. Mikula, P. Młynarz, Phytochemicals containing biologically active polyphenols as an effective agent against Covid-19-inducing coronavirus, J. Funct. Foods (2020) 104146, https://doi.org/10.1016/j.jff.2020.104146.

[52] Vardhan, S., Sahoo, S.K. In Silico ADMET and Molecular Docking Study on Searching Potential Inhibitors from Limonoids and Triterpenoids for COVID-19. arXiv preprint arXiv:2005.07955.

[53] N.M. O'Boyle, M. Banck, C.A. James, C. Morley, T. Vandermeersch, G. R. Hutchison, Open Babel: an open chemical toolbox, J. Cheminf. 3 (2011) 1–14.

[54] D.S. Goodsell, G.M. Morris, A.J. Olson, Automated docking of flexible ligands: applications of AutoDock, J. Mol. Recogn. 9 (1996) 1–5.

[55] O. Trott, A.J. Olson, AutoDock Vina, Improving the speed and accuracy of docking with a new scoring function, efficient optimization, and multithreading, J. Comput. Chem. 31 (2010) 455–461.

[56] M.L. Verdonk, J.C. Cole, M.J. Hartshorn, C.W. Murray, R.D. Taylor, Improved protein-ligand docking using GOLD, Proteins: Struct. Funct. Bioinf. 52 (2003) 609–623.

[57] S. Pronk, S. Pall, R. Schulz, P. Larsson, P. Bjelkmar, R. Apostolov, et al., GROMACS 4.5: a high-throughput and highly parallel open source molecular simulation toolkit, Bioinformatics 29 (2013) 845–854.

[58] K. Vanommeslaeghe, E. Hatcher, C. Acharya, S. Kundu, S. Zhong, J. Shim, et al., CHARMM general force field: a force field for drug-like molecules compatible with the CHARMM all-atom additive biological force fields, J. Comput. Chem. 31 (2009) 671–690.

[59] W.L. Jorgensen, J. Chandrasekhar, J.D. Madura, R.W. Impey, M.L. Klein, Comparison of simple potential functions for simulating liquid water, J. Chem. Phys. 79 (1983) 926–935.

[60] A. Toukmaji, C. Sagui, J. Board, T. Darden, Efficient particle-mesh Ewald based approach to fixed and induced dipolar interactions, J. Chem. Phys. 113 (2000) 10913–10927.

[61] H.J.C. Berendsen, J.P.M.v. Postma, W.F. van Gunsteren, A. DiNola, J.R. Haak, Molecular dynamics with coupling to an external bath, J. Chem. Phys. 81 (1984) 3684–3690.

[62] M. Parrinello, A. Rahman, Polymorphic transitions in single crystals: a new molecular dynamics method, J. Appl. Phys. 52 (1981) 7182–7190.

[63] J.A. Marsh, S.A. Teichmann, Relative solvent accessible surface area predicts protein conformational changes upon binding, Structure 19 (2011) 859–867.

[64] P.S. Srikumar, K. Rohini, P.K. Rajesh, Molecular dynamics simulations and principal component analysis on human laforin mutation W32G and W32G/K87A, Protein J. 33 (2014) 289–295.

[65] R. Kumari, R. Kumar, A. Lynn, g_mmpbsa–a GROMACS tool for high-throughput MM-PBSA calculations, J. Chem. Inf. Model. 54 (2014) 1951–1962.

[66] Y.N. Mabkhot, F. Alatibi, N.N. El-Sayed, S. Al-Showiman, N.A. Kheder, A. Wadood, et al., Antimicrobial activity of some novel armed thiophene derivatives and Petra/Osiris/Molinspiration (POM) analyses, Molecules 21 (2016).

[67] S.K. Srivastava, A.K.S. Rawat, M. Srivastava, S. Mehrotra, Pharmacognostic evaluation of the roots of Berberis chitria Lindl, Nat. Prod. Sci. 12 (2006) 19.

[68] D. Bhardwaj, N. Kaushik, Phytochemical and pharmacological studies in genus Berberis, Phytochemistry Rev. 11 (2012).

[69] C. Huang, Y. Wang, X. Li, L. Ren, J. Zhao, Y. Hu, et al., Clinical features of patients infected with 2019 novel coronavirus in Wuhan, China, Lancet 395 (2020) 497–506.

[70] A.J. Siddiqui, C. Danciu, S.A. Ashraf, A. Moin, R. Singh, M. Alreshidi, et al., Plants-derived biomolecules as potent antiviral phytomedicines: new insights on ethnobotanical evidences against coronaviruses, Plants 9 (2020) 1244.

[71] S. Jeon, M. Ko, J. Lee, I. Choi, S.Y. Byun, S. Park, et al., Identification of antiviral drug candidates against SARS-CoV-2 from FDA-approved drugs, Antimicrob. Agents Chemother. (2020).

[72] A. Agrawal, N.K. Jain, N. Kumar, G.T. Kulkarni, MOLECULAR DOCKING STUDY TO IDENTIFY POTENTIAL INHIBITOR OF COVID-19 MAIN PROTEASE ENZYME: AN IN-SILICO APPROACH, 2020.

[73] T. Belwal, I.D. Bhatt, R.S. Rawal, V. Pande, Microwave-assisted extraction (MAE) conditions using polynomial design for improving antioxidant phytochemicals in Berberis asiatica Roxb. ex DC. leaves, Ind. Crop. Prod. 95 (2016) 393–403.

[74] S. Lalani, C.L. Poh, Flavonoids as antiviral agents for Enterovirus A71 (EV-A71), Viruses 12 (2020) 184.

[75] V. Bajpai, A. Singh, K.R. Arya, M. Srivastava, B. Kumar, Rapid screening for the adulterants of Berberis aristata using direct analysis in real-time mass spectrometry and principal component analysis for discrimination, Food Addit. Contam. Part A Chem Anal Control Expo Risk Assess 32 (2015) 799–807.

[76] E. Petrera, A.G. NÁttolo, L.E. AlchÁ©, Antiviral action of synthetic stigmasterol derivatives on herpes simplex virus replication in nervous cells in vitro, BioMed Res. Int. 2014 (2014).

[77] F.S. Varghese, B. Thaa, S.N. Amrun, D. Simarmata, K. Rausalu, T.A. Nyman, et al., The antiviral alkaloid berberine reduces chikungunya virus-induced mitogen-activated protein kinase signaling, J. Virol. 90 (2016) 9743–9757.

[78] K. Hayashi, K. Minoda, Y. Nagaoka, T. Hayashi, S. Uesato, Antiviral activity of berberine and related compounds against human cytomegalovirus, Bioorg. Med. Chem. Lett 17 (2007) 1562–1564.

[79] A. Warowicka, R. Nawrot, A. Goździcka-Józefiak, Antiviral activity of berberine, Arch. Virol. 165 (2020) 1935–1945.

[80] C.C. Lai, C.K. Tan, Y.T. Huang, P.L. Shao, P.R. Hsueh, Current challenges in the management of invasive fungal infections, J. Infect. Chemother. 14 (2008) 77–85.

[81] K. Kaihatsu, M. Yamabe, Y. Ebara, Antiviral mechanism of action of epigallocatechin-3-O-gallate and its fatty acid esters, Molecules 23 (2018) 2475.

[82] A. Thawabteh, S. Juma, M. Bader, D. Karaman, L. Scrano, S.A. Bufo, et al., The biological activity of natural alkaloids against herbivores, cancerous cells and pathogens, Toxins 11 (2019) 656.

[83] J. Trivedi, A. Tripathi, D. Chattopadhyay, D. Mitra, Plant-Derived molecules in managing HIV infection, in: New Look to Phytomedicine, Elsevier, 2019, pp. 273–298.

[84] S. Pushpakom, F. Iorio, P.A. Eyers, K.J. Escott, S. Hopper, A. Wells, et al., Drug repurposing: progress, challenges and recommendations, Nat. Rev. Drug Discov. 18 (2019) 41–58.

[85] G. Bupesh, R.S. Raja, K. Saravanamurali, V.S. Kumar, N. Saran, M. Kumar, et al., Antiviral activity of ellagic acid against envelope proteins from Dengue virus through insilico docking, Int. J. Drug Dev. Res. 6 (2014) 975–9344.

[86] Q. Cui, R. Du, M. Anantpadma, A. Schafer, L. Hou, J. Tian, et al., Identification of ellagic acid from plant Rhodiola rosea L. as an anti-Ebola virus entry inhibitor, Viruses 10 (2018) 152.

[87] M. Le Donne, M. Lentini, A. Alibrandi, V. Salimbeni, F. Mazzeo, O. Triolo, et al., Antiviral activity of ellagic acid and Annona muricata in cervical HPV related pre-neoplastic lesions: a randomized trial, J. Funct. Foods 35 (2017) 549–554.

[88] F.R. Bhuiyan, S. Howlader, T. Raihan, M. Hasan, Plants metabolites: possibility of natural therapeutics against the COVID-19 pandemic, Front. Med. 7 (2020) 444.

[89] H. Andola, R. Rawal, I.D. Bhatt, Antioxidants in fruits and roots of Berberis asiatica Rox. ex. DC.: a highly valued Himalayan plant, Natl. Acad. Sci. Lett. 31 (2008) 337–340.

[90] M.G. Salas, A.M.R. Estilla, J.A.M. Chávez, S.A.L. Sepúlveda, R.R. Herrera, C.N. A. GonzÁ¡lez, P420 gallic acid has antiviral effect against hepatitis C virus (HCV), which is mediated by its antioxidant activity, J. Hepatol. 60 (2014) S208.

[91] J.M.l. Kratz, C.R. Andrighetti-FrÁ¶hner, D.J. Kolling, P.C.s. Leal, C.u.C.s. Cirne-Santos, R.A. Yunes, et al., Anti-HSV-1 and anti-HIV-1 activity of gallic acid and pentyl gallate, Mem. Inst. Oswaldo Cruz 103 (2008) 437–442.

[92] J.M.l. Kratz, C.R. Andrighetti-FrÁ¶hner, P.C. Leal, R.J. Nunes, R.A. Yunes, E. Trybala, et al., Evaluation of anti-HSV-2 activity of gallic acid and pentyl gallate, Biol. Pharm. Bull. 31 (2008) 903–907.

[93] B. Á–zÁ§elik, M. Kartal, I. Orhan, Cytotoxicity, antiviral and antimicrobial activities of alkaloids, flavonoids, and phenolic acids, Pharmaceut. Biol. 49 (2011) 396–402.

[94] H. Utsunomiya, M. Ichinose, K. Ikeda, M. Uozaki, J. Morishita, T. Kuwahara, et al., Inhibition by caffeic acid of the influenza A virus multiplication in vitro, Int. J. Mol. Med. 34 (2014) 1020–1024.

[95] C.M. Gurmachhan, U. Tandukar, N. Shrestha, P.B. Lakhey, C.P. Pokhrel, Antibacterial and phytochemical studies of bark extract of Berberisasiatica Roxb. Ex. DC. And Myrica esculenta Buch.-Ham ex. D. Don, J. Plant Res. 17 (2019) 139–146.

[96] N.L. Sheehan, R.P.G. Van Heeswijk, B.C. Foster, H. Akhtar, N. Singhal, I. Seguin, et al., The effect of Î²-carotene supplementation on the pharmacokinetics of nelfinavir and its active metabolite M8 in HIV-1-infected patients, Molecules 17 (2012) 688–702.

[97] R.B. Turner, K.A. Biedermann, J.M. Morgan, B. Keswick, K.D. Ertel, M.F. Barker, Efficacy of organic acids in hand cleansers for prevention of rhinovirus infections, Antimicrob. Agents Chemother. 48 (2004) 2595–2598.

[98] M.J. Kwon, H.M. Shin, H. Perumalsamy, X. Wang, Y.-J. Ahn, Antiviral effects and possible mechanisms of action of constituents from Brazilian propolis and related compounds, J. Apicult. Res. 59 (2020) 413–425.

[99] P.E. Stamets, Antiviral Activity from Medicinal Mushrooms and Their Active Constituents, Google Patents, 2016.

[100] H. Martens, T. Naes, Multivariate Calibration, John Wiley & Sons, 1992.

[101] R. Shukla, P.B. Chetri, A. Sonkar, M.Y. Pakharukova, V.A. Mordvinov, T. Tripathi, Identification of novel natural inhibitors of Opisthorchis felineus cytochrome P450 using structure-based screening and molecular dynamic simulation, J. Biomol. Struct. Dyn. 36 (2018) 3541–3556.

[102] R. Shukla, H. Shukla, T. Tripathi, Activity loss by H46A mutation in Mycobacterium tuberculosis isocitrate lyase is due to decrease in structural plasticity and collective motions of the active site, Tuberculosis 108 (2018) 143–150.

[103] Y.M. Arabi, A. Alothman, H.H. Balkhy, A. Al-Dawood, S. AlJohani, S. Al Harbi, et al., Treatment of Middle East respiratory syndrome with a combination of lopinavir-ritonavir and interferon-Î²1b (MIRACLE trial): study protocol for a randomized controlled trial, Trials 19 (2018) 1–13.

[104] S. Bimonte, A. Crispo, A. Amore, E. Celentano, A. Cuomo, M. Cascella, Potential antiviral drugs for SARS-cov-2 treatment: Preclinical findings and ongoing clinical research, In Vivo 34 (2020) 1597–1602.

[105] Y. Xian, J. Zhang, Z. Bian, H. Zhou, Z. Zhang, Z. Lin, et al., Bioactive natural compounds against human coronaviruses: a review and perspective, Acta Pharm. Sin. B (2020).

[106] T. Joshi, P. Sharma, T. Joshi, H. Pundir, S. Mathpal, S. Chandra, Structure-based screening of novel lichen compounds against SARS Coronavirus main protease (Mpro) as potentials inhibitors of COVID-19, Mol. Divers. (2020) 1–13.

[107] D. Bhardwaj, N. Kaushik, Phytochemical and pharmacological studies in genus Berberis, Phytochemistry Rev. 11 (2012) 523–542.

Tanuja Joshi is a researcher at the Department of Botany, Soban Singh Jeena University, Almora, Uttarakhand, India. She is working in the area of structural bioinformatics and Enzyme Technology.

Sunaullah Bhat is a researcher at the Department of Zoology, Kumaun University, Nainital Uttarakhand, India. He is working in the area of drug discovery.

Hemlata Pundir is a researcher at the Department of Botany, D.S.B Campus, Kumaun University, Nainital, Uttarakhand, India. She is working in the area of bioinformatics and Antiviral Research.

Subhash Chandra is a Professor at Computational Biology & Biotechnology Laboratory, Department of Botany, Soban Singh Jeena University, Almora, Uttarakhand, India. He is working in the area of vaccine development, data mining, artificial intelligence, computational biology, viral informatics, and drug discovery.